ELSEVIER

Journal of Organometallic Chemistry 514 (1996) 125–136

Journal of Organometallic Chemistry

Coordination chemistry of 1,1'-bis(2-pyridyl)ferrocene in palladium(II) and platinum(II) complexes and reaction of (BPF)Pd(Me)Cl with CO. X-ray structure of (1,1'-bis(2-pyridyl)ferrocene)Pd(Me)Cl and (1,1'-bis(2-pyridyl)ferrocene)$[PtCl_2(CH_2=CH_2)]_2$

Johannes G.P. Delis [a], Piet W.N.M. van Leeuwen [a,*], Kees Vrieze [a], Nora Veldman [b], Anthony L. Spek [b,1], Jan Fraanje [c], Kees Goubitz [c,2]

[a] *Anorganisch Chemisch Laboratorium, J.H. van't Hoff Instituut, Universiteit van Amsterdam, Nieuwe Achtergracht 166, NL-1018 WV Amsterdam, Netherlands*

[b] *Bijvoet Center for Biomolecular Research, Vakgroep Kristal- en Structuurchemie, Universiteit Utrecht, Padualaan 8, NL-3584 CH Utrecht, Netherlands*

[c] *Laboratorium voor Kristallografie, J.H. van't Hoff Instituut, Universiteit van Amsterdam, Nieuwe Achtergracht 166, NL-1018 WV Amsterdam, Netherlands*

Received 17 August 1995

Abstract

The coordination chemistry of the ligand 1,1'-bis(2-pyridyl)ferrocene (BPF) towards palladium and platinum has been studied. The very stable complexes (BPF)Pd(Me)Cl and BPF$[PtCl_2(CH_2=CH_2)]_2$ have been synthesized from (COD)Pd(Me)Cl and Zeise's salt respectively and characterized by ^{1}H-, ^{13}C-NMR, elemental analysis and single crystal X-ray determination. The crystals of (BPF)Pd(Me)Cl crystallize in the monoclinic space group $C2/c$ (No. 15) with $a = 17.4681(9)$, $b = 9.1112(6)$, $c = 27.598(2)$ Å, $\beta = 96.926(5)°$, $V = 4360.3(5)$ Å^3, $Z = 8$. The structure refinement converged to $R_1 = 0.042$ for 3541 $F_o > 4\sigma(F_o)$ and $wR_2 = 0.084$ for all 4982 unique reflections. The X-ray structure shows a square planar palladium complex with the ligand coordinated in a bidentate way with a relatively large bite angle of 84.48(13)°. The crystals of BPF$[PtCl_2(CH_2=CH_2)]_2$ have the space group $P2_1/n$ with $a = 13.8584(9)$, $b = 13.128(3)$, $c = 14.807(1)$ Å and $\beta = 90.13(1)°$, $V = 2693.9(7)$ Å^3, $Z = 4$. The structure refinement converged to $R = 0.043$ for 4310 observed reflections. This structure contains two $PtCl_2(CH_2=CH_2)$ fragments bridged by one BPF ligand. A fast CO insertion occurs into the palladium–methyl bond of the complex (BPF)Pd(Me)Cl. When the product of this reaction, (BPF)Pd(C(O)Me)Cl, is kept under an atmosphere of ^{13}CO, low temperature NMR and IR measurements show the presence of four complexes, which are (BPF)Pd(C(O)Me)Cl and probably (BPF)Pd(C(O)Me)(CO)Cl, *cis*- and *trans*-$Pd_2(CO)_2(C(O)Me)_2Cl_2$. Both the complexes (BPF)Pd(Me)Cl and (BPF)Pd(C(O)Me)Cl show a fluxional behaviour of the coordinated BPF ligand in solution on the NMR time scale, which involves the interconversion of two enantiomers of the complexes and the exchange of the two pyridyl groups of the ligand. BPF$[PtCl_2(CH_2=CH_2)]_2$, in which the ethylene is tightly coordinated to the metal centre, reacts with an additional BPF ligand to give the four-coordinated complex (BPF)$PtCl_2(CH_2=CH_2)$.

Keywords: Platinum; Palladium; Ferrocene; Insertion; Carbon monoxide

1. Introduction

The CO insertion reaction is an important step in copolymerization of alkenes and carbon monoxide [1–6]. In our and other laboratories CO insertions into palladium–carbon bonds of complexes containing bidentate phosphine [7–9], bidentate nitrogen [10], nitrogen–phosphine [11] and also terdentate nitrogen ligands [12] are being investigated extensively. Previous studies on a series of (P–P)Pd(Me)X complexes showed that the type of phosphine ligand has a large effect on the CO insertion rate [7]. The highest reaction rate is found for the bidentate ligand $(C_6H_5)_2P-(CH_2)_3-P(C_6H_5)_2$

* Corresponding author.

[1] Corresponding author re. X-ray structure of (BPF)Pd(Me)Cl (2).

[2] Corresponding author re. X-ray structure of BPF$[PtCl_2(CH_2=CH_2)]_2$ (3).

SSDI 0022-328X(95)05992-X

(dppp), which is believed to originate from a combination of flexibility and a relatively large bite angle of the ligand.

Since late-transition metals are soft Lewis acids, the soft Lewis base phosphorus ligands provide very robust metal complexes, while the harder nitrogen ligands form generally less stable complexes. Nevertheless, many palladium complexes containing nitrogen-based ligands have been synthesized and CO insertions into palladium–carbon bonds of these complexes have been carried out [10,13–15]. Unexpectedly, a faster reaction rate is observed when, instead of bidentate phosphine ligands, bidentate nitrogen ligands are used [13]. Since for flexible diphosphine ligands with a large bite angle high insertion rates are found it is rather surprising that, not only for flexible bidentate nitrogen ligands but also for very rigid bidentate nitrogen ligands, which both have small bite angles (76–80°), faster CO insertions are observed [10,13,16].

Since we are interested in studying the influence of both the flexibility and the bite angle of bidentate ligands on CO insertions, it appeared to us that it would be timely to investigate the bidentate nitrogen ligand 1,1'-bis(2-pyridyl)ferrocene (BPF). This ligand is very flexible as it also coordinates with a large bite angle, e.g. in the complex $[Ag(BPF)ClO_4]_2$ (N1–Ag–N2 = 163.1(1)°) [17]. In this article we will report the coordination chemistry of the ligand BPF towards palladium and platinum and furthermore the reactivity of the complex towards insertion reactions in view of its flexibility and propensity to coordinate with a large bite angle.

2. Experimental

2.1. Materials and apparatus

All manipulations were carried out in an atmosphere of purified, dry nitrogen by using standard Schlenk techniques. Solvents were dried and stored under nitrogen. ^{1}H-NMR and ^{13}C-NMR were recorded on a Bruker AMX 300 (300.13 and 75.48 MHz respectively). Chemical shift values are in ppm relative to TMS. Low temperature IR spectra were recorded with a thermostatic IR cell on a Bio-Rad FTS-7 spectrometer. Elemental analyses were carried out by Dornis u. Kolbe Mikroanalytisches Laboratorium, Mülhlheim a.d. Ruhr, Germany. Dibal-H was purchased and used without purification. $FcLi_2$/TMEDA [18], (COD)PdMeCl [19] and $K[PtCl_3(CH_2=CH_2)]$ [20] were synthesized according to previously reported procedures.

2.2. Synthesis of 1,1'-bis(2-pyridyl)ferrocene, BPF (1)

$FcLi_2$/TMEDA (4.0 g, 13 mmol) was dissolved in THF (100 ml) and cooled to 0°C. $ZnCl_2$ (25.6 ml, 25.6 mmol, 1.0 M in Et_2O) dissolved in THF (60 ml) and cooled to 0°C was added and the orange solution was warmed to room temperature. A yellow suspension was formed within 1 h. In a separate flask $(PPh_3)_2PdCl_2$ (380 mg, 0.60 mmol) was suspended in THF (20 ml), to which Dibal-H (1.25 ml, 1.25 mmol, 1 M in THF) was added dropwise. This gave a homogeneous dark solution of $(PPh_3)_2Pd$ which was added to the 1,1'-bis(zinc-chloride)ferrocene via a cannula. 2-Bromopyridine (2.5 g, 32 mmol) was added dropwise to the reaction mixture. A solution of NaOH (10 g, 0.25 mol) in water (100 ml) was added to the solution after 25 h. The organic layer was separated from the water fraction, which was extracted twice with CH_2Cl_2 (100 ml). The organic layers were dried with Mg_2SO_4. The solvent was evaporated and the residue brought upon a column with neutral Al_2O_3. Elution with diethylether yielded a yellow–orange fraction containing (2-pyridyl)ferrocene. Elution with CH_2Cl_2 yielded an orange fraction containing BPF. The product BPF was recrystallized from diethylether at −40°C. Yield 2.4 g (7.2 mmol; 55%).

^{1}H-NMR (300 MHz, $CDCl_3$) δ 8.36 (d, ^3J = 5.3 Hz, 2, H5; H15), 7.35 (dt, ^3J = 8.6 Hz, ^4J = 1.9 Hz, 2, H3; H13), 7.08 (d, ^3J = 8.6 Hz, 2, H2; H12), 6.99 (ddd, ^3J = 8.6 Hz, ^3J = 5.3 Hz, ^4J = 1.0 Hz, 2, H4; H14), 4.83 (t, ^3J = 2.1 Hz, 4, H7; H9; H17; H20), 4.33 (t, ^3J = 2.1 Hz, 4, H8; H10; H18; H19).

^{13}C-NMR (75.48 MHz, $CDCl_3$) δ 157.9 (Cl; C11), 149.7 (C5; C15), 136.3 (C3; C13), 120.7 (C4; C14), 120.6 (C2; C12), 71.6, 68.9, 85.5 (C_5H_4).

2.3. Synthesis of (1,1'-bis(2-pyridyl)ferrocene)chloromethylpalladium(II), (BPF)Pd(Me)Cl (2)

(COD)Pd(Me)Cl (250 mg, 0.94 mmol) and BPF (330 mg, 0.97 mmol) were dissolved in toluene (20 ml). The orange suspension, which was formed after 30 min, was centrifuged and washed twice with diethylether (20 ml) to yield an orange powder (424 mg, 0.86 mmol, 91%). Crystals suitable for X-ray analysis were obtained by slow diffusion of diethylether in a solution of the product in CH_2Cl_2 at −20°C.

^{1}H-NMR (300 MHz, $CDCl_3$ 223 K) δ 9.10, 9.16 (d, ^3J = 5.0 Hz, 2, H5; H15), 7.44, 7.37 (t, ^3J = 7.6 Hz, 2, H3; H13), 7.21–7.05 (m, 4, H2; H12, H4; H14), 6.63, 6.46 (s, 2, H7; H20), 4.65, 4.58, 4.51, 4.43 (s, 6, H9; H17, H8, H10, H18; H19), 0.91 (s, 3, Pd–Me).

^{13}C-NMR (75.48 MHz, $CDCl_3$ 264 K) δ 158.5, 160.5 (C1; C11), 151.1, 152.9 (C5; C15), 137.3, 137.5 (C3; C13), 125.1, 125.9 (C2; C12), 122.0, 122.5, (C4; C14), 85.4, 86.2, 72.3, 75.4, 71.6, 72.0, 70.1, 70.5, 66.5, 66.8 (C_5H_4), −6.2 (Pd–Me).

Anal. Found: C, 49.87; H, 3.81; N, 5.55. $C_{21}H_{19}ClFeN_2Pd$. Calc.: C, 49.43; H, 3.42; N, 5.42.

2.4. Synthesis of (1,1'-bis(2-pyridyl)ferrocene)bis[dichloro(η^2-ethylene)platinum(II)], BPF[PtCl$_2$(CH$_2$=CH$_2$)]$_2$ (3)

K[PtCl$_3$(CH$_2$=CH$_2$)] (73.6 mg, 0.21 mmol) and BPF (114.8 mg, 0.33 mmol) were dissolved in CH_2Cl_2 (30 ml) and stirred for 4 h. The solution was filtered and the volume of the solution concentrated to 5 ml. Diethylether was added to the solution and the product (160 mg, 0.17 mmol, 82%) was collected by centrifugation. Crystals suitable for X-ray analysis were obtained by slow diffusion of diethylether in a solution of the product in CH_2Cl_2.

^{1}H-NMR (300 MHz, $CDCl_3$) δ 8.48 (d, ^3J = 6.6 Hz, $^3J_{Pt-H}$ = 30 Hz, 2, H5; H15), 7.56 (d, ^3J = 8.9 Hz, 2, H2; H12), 7.35 (dt, ^3J = 8.9 Hz, ^4J = 1.7 Hz, 2, H3; H13), 7.04 (t, ^3J = 6.6 Hz, 2, H4; H14) 5.75 (t, ^3J = 2.1 Hz, 4, H7; H20, H9; H17), 4.67 (t, ^3J = 2.1 Hz, 4, H8; H10, H18; H19), 4.73 (s, $^3J_{Pt-H}$ = 62 Hz, 8, $H_2C=CH_2$).

^{13}C-NMR (75.48 MHz, $CDCl_3$) δ 159.0 (C1; C11), 149.8 (C5; C15), 139.4 (C3; C13), 129.5 (C2; C12), 122.4 (C4; C14), 86.5, 72.8, 71.9 (C_5H_4), 74.5 (C=C).

Anal. Found: C, 30.92; H, 2.64; N, 2.94. $C_{24}H_{24}Cl_4FeN_2Pt_2$. Calc.: C, 31.05; H, 2.61; N, 3.01.

2.5. Synthesis of (1,1'-bis(2-pyridyl)ferrocene)acetylchloropalladium(II), (BPF)Pd(C(O)Me)Cl (4)

CO was bubbled through a solution of (BPF)Pd(Me)Cl (105 mg, 0.21 mmol) in CH_2Cl_2 (20 ml) for 5 min, after which the solution was filtered. The solution was

Table 1
Crystal and refinement data for (BPF)Pd(Me)Cl (2) and [PtCl$_2$(CH$_2$=CH$_2$)]$_2$BPF (3)

	2	3
Crystal data		
Chemical formula	$C_{21}H_{19}ClFeN_2Pd \cdot CH_2Cl_2$	$C_{24}H_{24}Cl_4FeN_2Pt_2$
Molecular weight	582.05	928.3
Crystal system	monoclinic	monoclinic
Space group	$C2/c$ (No. 15)	$P2_1/n$ (No. 14)
a (Å)	17.4681(9)	13.8584(9)
b (Å)	9.1112(6)	13.128(3)
c (Å)	27.598(2)	14.807(1)
β (°)	96.926(5)	90.13(1)
V (Å^3)	4360.3(5)	2693.9(7)
D_{calc} (g cm^{-3})	1.773	2.289
Z	8	4
F(000)	2320	1728
μ (cm^{-1})	18.7 (Mo K α)	274.3 (Cu K α)
Crystal size (mm^3)	0.13 × 0.13 × 0.43	0.05 × 0.25 × 0.60
Data collection		
T (K)	150	293
θ_{min}, θ_{max} (°)	1.5, 27.5	2.5, 76.3
Wavelength (Å)	0.71073 (Mo K α) (graphite-monochromated)	1.54184 (Cu K α) (graphite-monochromated)
Scan type	ω	ω–2θ
X-ray exposure time (h)	19.3	60
Linear decay (%)	2	0
Reference reflection	−2 2 5, 4 2 5, −5 1 2	1 4 0, 0 2 3
Data set	−22:22, 0:11, −31:35	−17:17, 0:14, 0:18
Total data	8461	5349
Total unique data	4989	5349
DIFABS correction range	0.84–1.29	0.64–2.27
Refinement		
No. of refined parameters	263	396
Final R [a]	0.042 [3541 $F_o > 4\sigma(F_o)$]	0.043 [4310 $F_o > 5\sigma(F_o)$]
Final wR_2 [b]	0.084 [4982 data]	
Final Rw [c]		0.065 [4310 data]
Goodness of fit	1.016	
w^{-1} [d]	$\sigma^2(F^2) + (0.0923P)^2$	$8.5 + F_o + 0.0067F_o^2$
$(\Delta/\sigma)_{max}$	0.001	0.46
Min. and max. ρ (e Å^{-3})	−0.56, 0.54	−1.9, 1.6

[a] $R_1 = \Sigma(||F_o| - |F_c||)/\Sigma|F_o|$. [b] $wR_2 = [\Sigma[w(F_o^2 - F_c^2)^2]/\Sigma[w(F_o^2)^2]]^{0.5}$. [c] $Rw = [\Sigma[w(||F_o| - |F_c||)^2]/\Sigma[w(F_o^2)]]^{0.5}$. [d] $P = (\max(F_o^2, 0) + 2F_c^2)/3$.

concentrated to 5 ml and ether (20 ml) was added. The crystalline material (99 mg, 0.19 mmol, 90%) was collected by centrifugation.

^{1}H-NMR (300 MHz, $CDCl_3$ 219 K) δ 9.24, 9.06 (d, ^3J = 5.0 Hz, 2, H5; H15), 7.43, 7.41 (t, ^3J = 7.7 Hz, 2, H3; H13), 7.19–7.02 (m, 4, H2; H12, H4; H14), 6.79, 6.62 (s, H7; H20), 4.70, 4.59, 4.55, 4.44 (s, 6, H9; H17, H8; H10, H18; H19), 2.78 (s, 3, Pd–C(O)Me).

^{13}C-NMR (75.48 MHz, $CDCl_3$ 219 K) δ 158.0, 160.2 (C1; C11), 150.7, 152.0 (C5; C15), 137.9, 138.3 (C3; C13), 124.2, 125.9, (C2; C12), 122.2, 122.7, (C4; C14), 85.5, 85.4, 74.3, 72.6, 71.9, 71.0, 70.5, 66.9 (C_5H_4), 35.7 (Pd–C(O)*Me*), 226.9 (Pd–*C(O)*Me).

Anal. Found: C, 49.94; H, 3.57; N, 5.38. $C_{22}H_{19}ClFeN_2OPd$. Calc.: C, 50.32; H, 3.64; N, 5.33.

2.6. Low temperature NMR experiments of (BPF)Pd-(Me)Cl under ^{13}CO atmosphere

(BPF)Pd(Me)Cl (5.0 mg, 0.01 mmol) was dissolved in $CDCl_3$ (0.6 ml) and transferred to an NMR tube. ^{13}CO was bubbled through the solution for 1 min, after which the tube was closed. ^{1}H and ^{13}C spectra were measured at 223 K.

^{13}C NMR (of the carbonyl region, 223 K): δ 226.9; 218.1; 214.1; 213.9; 184.9; 174.5; 171.7; 171.6.

2.7. X-ray structure determination of 2

An orange–red crystal (0.13 × 0.13 × 0.43 mm^3, cut to size and covered in inert oil) was mounted on top of a Lindermann-glass capillary and transferred into the cold nitrogen stream on an Enraf-Nonius CAD4-T diffractometer on rotating anode. Accurate unit-cell parameters and an orientation matrix were determined from the setting angles of 25 reflections (SET4 [21]) in the range $9.9° < \theta < 14.0°$. Reduced-cell calculations did not indicate higher lattice symmetry [22]. Crystal data and details on data collection and refinement are given in Table 1.

Data were corrected for Lp effects and for a linear decay of 2% of the periodically measured reference reflections. An empirical absorption/extinction correction was applied (DIFABS [23] as implemented in PLATON [24]). The structure was solved by automated Patterson methods and subsequent difference Fourier techniques, DIRDIF-92 [25]. Refinement on F^2 was carried out by full-matrix least-squares techniques (SHELXL-93 [26]); no observance criterion was applied during refinement. Non-hydrogen atoms were refined with anisotropic thermal parameters. The hydrogen atoms were refined with fixed isotropic thermal parameters related to the value of the equivalent isotropic thermal parameter of their

Table 2
Final coordinates and equivalent isotropic thermal parameters of the non-hydrogen atoms for (BPF)Pd(Me)Cl (2) (with e.s.d.s in parentheses)

Atom	x	y	z	U_{eq} (Å^2)
Pd(1)	0.36730(2)	0.37614(3)	0.13903(1)	0.0188(1)
Fe(1)	0.26821(3)	0.05761(6)	0.19201(2)	0.0181(2)
Cl(1)	0.27953(6)	0.56339(12)	0.11915(4)	0.0299(3)
N(1)	0.4519(2)	0.2167(4)	0.15253(12)	0.0204(12)
N(2)	0.3237(2)	0.2355(4)	0.07711(12)	0.0216(12)
C(1)	0.4455(2)	0.0862(4)	0.17549(15)	0.0192(12)
C(2)	0.4988(2)	−0.0260(5)	0.1702(2)	0.0281(16)
C(3)	0.5582(2)	−0.0049(5)	0.1424(2)	0.0306(16)
C(4)	0.5653(2)	0.1295(5)	0.1208(2)	0.0305(14)
C(5)	0.5118(2)	0.2366(5)	0.1266(2)	0.0264(14)
C(6)	0.3856(2)	0.0644(4)	0.20742(14)	0.0192(12)
C(7)	0.3514(2)	0.1739(5)	0.23462(14)	0.0217(12)
C(8)	0.3014(2)	0.1034(5)	0.26437(14)	0.0238(14)
C(9)	0.3045(2)	−0.0488(5)	0.2557(2)	0.0254(12)
C(10)	0.3567(2)	−0.0744(5)	0.2210(2)	0.0249(12)
C(11)	0.2825(2)	0.1086(5)	0.07806(14)	0.0213(12)
C(12)	0.2798(2)	0.0087(5)	0.0404(2)	0.0289(14)
C(13)	0.3167(3)	0.0382(6)	0.0000(2)	0.0349(16)
C(14)	0.3554(3)	0.1692(6)	−0.0019(2)	0.0351(16)
C(15)	0.3579(3)	0.2633(5)	0.0372(2)	0.0296(16)
C(16)	0.2367(2)	0.0847(4)	0.11829(15)	0.0188(12)
C(17)	0.2104(2)	−0.0538(5)	0.1346(2)	0.0240(12)
C(18)	0.1605(2)	−0.0269(5)	0.1707(2)	0.0259(14)
C(19)	0.1563(2)	0.1266(5)	0.17752(15)	0.0214(12)
C(20)	0.2031(2)	0.1963(5)	0.14554(14)	0.0213(12)
C(21)	0.4197(2)	0.5103(5)	0.1927(2)	0.0252(12)
Cl(2)	0.41172(9)	0.6676(2)	−0.00548(6)	0.0654(6)
Cl(3)	0.51548(7)	0.64315(15)	0.08467(5)	0.0453(4)
C(22)	0.4291(3)	0.7209(6)	0.0564(2)	0.0443(17)

Table 3
Bond distances (Å) in (BPF)Pd(Me)Cl (2) (with e.s.d.s in parentheses)

Pd–C11	2.3150(11)	Pd–N1	2.074(4)	Pd–N2	2.197(3)
Pd–C21	2.049(5)	N1–C1	1.358(5)	N1–C5	1.349(5)
N2–C11	1.364(6)	N2–C15	1.339(6)	C1–C2	1.402(5)
C1–C6	1.461(5)	C2–C3	1.376(6)	C3–C4	1.347(7)
C4–C5	1.374(6)	C11–C12	1.378(7)	C12–C13	1.380(7)
C13–C14	1.376(8)	C14–C15	1.375(8)		

carrier atoms by a factor of 1.5 for the methyl–hydrogen atoms and a factor of 1.2 for the other hydrogen atoms. In the final stages of refinement an (independent) small void remained of approximately 15.2 Å^3 on the special position 0.5, 0, 0. However, no residual density was found in that area (PLATON/SQUEEZE [27]). Weights were optimized in the final refinement cycles. Neutral atom scattering factors and anomalous dispersion corrections were taken from *International Tables for Crystallography* [28].

Geometrical calculations and the illustration were performed with PLATON [24]; all calculations were performed on a DEC5000/125. Positional parameters are listed in Table 2 for **2**, bond distances in Table 3 and bond angles in Table 4.

2.8. X-ray structure determination of 3

A crystal with approximate dimensions 0.05 × 0.25 × 0.60 mm^3 was used for data collection on an Enraf-Nonius CAD-4 diffractometer with graphite-monochromated Cu Kα radiation and ω–2θ scan. Crystal data and details on data collection and refinement are given in Table 1. A total of 5349 unique reflections were measured within the range $-17 \le h \le 17$, $0 \le k \le 14$, $0 \le l \le 18$. Of these, 4310 were above the significance level of $2.5\sigma(I)$. The maximum value of $(\sin\theta)/\lambda$ was 0.63 Å^{-1}. Two reference reflections (1 4 0, 0 2 3) were measured hourly and showed no decrease during the 60 h collecting time. Unit-cell parameters were refined by a least-squares fitting procedure using 23 reflections with $81° < 2\theta < 88°$. Corrections for Lorentz and polarisation effects were applied. The structure was solved by the PATTY/ORIENT/PHASEX option of the DIRDIF-91 program system [29]. The hydrogen atom positions were calculated. Full-matrix least-squares refinement on F, anisotropic for the non-hydrogen atoms and isotropic for the hydrogen atoms, restraining the latter in such a way that the distance on their carrier remained constant at approximately 1.09 Å, converged to $R = 0.043$, $Rw = 0.065$, $(\Delta/\sigma)_{max} = 0.46$. A weighting scheme $w = (8.5 + F_o + 0.0067F_o^2)^{-1}$ was used. An empirical absorption correction (DIFABS [23]) was applied, with coefficients in the range 0.64–2.27. The secondary isotropic extinction coefficient [30,31] refined to $G = 0.017(3)$. A final difference Fourier map revealed a residual electron density between −1.9 and 1.6 Å^{-3} in the vicinity of the heavy atoms. Scattering factors were taken from Refs. [32,33]. The anomalous scattering of Fe, Pt and Cl was taken into account. All calculations were performed with XTAL [34], unless stated otherwise. Positional parameters are listed in Table 5 for **3**, bond distances in Table 6 and bond angles in Table 7.

For both structures, determination tables of H-atom coordinates, thermal parameters and complete lists of bond lengths and angles have been deposited at the Cambridge Crystallographic Data Centre.

3. Results and discussion

3.1. Synthetic results

3.1.1. BPF (1)

An improved method to synthesize the ligand 1,1′-bis(2-pyridyl)ferrocene (BPF, **1**) was necessary since earlier reports mentioned a low yield. The ligand BPF was obtained by reaction of dilithioferrocene/TMEDA with $ZnCl_2$ and subsequent reaction with 2-bromopyridine in the presence of a catalytic amount of $Pd(PPh_3)_2$ (5%) which was formed by reducing $(PPh_3)_2$ $PdCl_2$ with two equivalents of Dibal-H (Scheme 1) [35].

Table 4
Bond angles (°) in (BPF)Pd(Me)Cl (2) (with e.s.d.s in parentheses)

C11–Pd–N2	95.04(10)	C11–Pd–C21	87.54(12)	N1–Pd–N2	84.48(13)
N1–Pd–C21	92.38(15)	Pd–N1–C1	126.9(3)	Pd–N1–C5	113.1(3)
C1–Pd–C5	118.5(4)	Pd–N2–C11	127.9(3)	Pd–N2–C15	112.5(3)
C11–N2–C15	117.7(4)	N1–C1–C2	119.8(4)	C1–C2–C3	120.7(4)
C2–C3–C4	118.7(4)	C3–C4–C5	119.0(4)	N1–C5–C4	123.3(4)
N2–C11–C12	121.0(4)	C11–C12–C13	120.3(4)	C12–C13–C14	118.6(5)
C13–C14–C15	118.7(5)	N2–C15–C14	123.5(4)		

Table 5
Final coordinates and equivalent isotropic thermal parameters of the non-hydrogen atoms for (BPF)[$PtCl_2(CH_2=CH_2)$]$_2$ (3) (with e.s.d.s in parentheses)

Atom	x	y	z	U_{eq} (Å^2)
Pt(1)	0.63596(3)	0.31512(3)	0.43771(3)	0.0349
Pt(2)	0.65150(3)	0.22759(3)	−0.11696(2)	0.0341
Fe	0.83839(9)	0.28985(12)	0.16353(9)	0.0309
Cl(1)	0.6952(3)	0.1691(3)	0.5004(2)	0.0655
Cl(2)	0.5686(3)	0.4571(3)	0.3740(2)	0.0850
Cl(3)	0.5943(2)	0.0813(2)	−0.05109(19)	0.0524
Cl(4)	0.6987(2)	0.3783(3)	−0.1813(2)	0.0595
N(1)	0.5901(6)	0.2340(7)	0.3249(5)	0.0372
N(2)	0.5966(6)	0.3085(6)	−0.0084(5)	0.0324
C(1)	0.6505(6)	0.2041(7)	0.2601(6)	0.0289
C(2)	0.6181(8)	0.1433(9)	0.1897(7)	0.0436
C(3)	0.5222(9)	0.1128(11)	0.1865(8)	0.0624
C(4)	0.4621(8)	0.1451(12)	0.2535(8)	0.0581
C(5)	0.4983(7)	0.2049(11)	0.3225(8)	0.0544
C(6)	0.7542(6)	0.2345(8)	0.2651(6)	0.0320
C(7)	0.7944(7)	0.3296(9)	0.2914(7)	0.0418
C(8)	0.8982(7)	0.3195(9)	0.2896(7)	0.0420
C(9)	0.9190(8)	0.2202(12)	0.2606(7)	0.0569
C(10)	0.8312(7)	0.1658(9)	0.2461(6)	0.0427
C(11)	0.6501(6)	0.3521(7)	0.0551(6)	0.0299
C(12)	0.6067(8)	0.4131(9)	0.1215(7)	0.0457
C(13)	0.5086(9)	0.4266(11)	0.1235(8)	0.0620
C(14)	0.4547(8)	0.3812(12)	0.0593(8)	0.0605
C(15)	0.4988(7)	0.3248(9)	−0.0046(7)	0.0427
C(16)	0.7565(6)	0.3362(8)	0.0570(6)	0.0347
C(17)	0.8072(8)	0.2426(11)	0.0347(6)	0.0495
C(18)	0.9066(8)	0.2628(14)	0.0439(8)	0.0605
C(19)	0.9201(7)	0.3643(14)	0.0686(9)	0.0698
C(20)	0.8263(9)	0.4108(10)	0.0800(8)	0.0536
C(21)	0.6381(14)	0.3904(13)	0.5681(10)	0.0775
C(22)	0.7247(14)	0.4029(16)	0.5258(12)	0.0944
C(23)	0.6021(9)	0.1502(11)	−0.2459(8)	0.0565
C(24)	0.7499(11)	0.1418(13)	−0.2004(9)	0.0687

The red crystalline product was obtained in 55% yield, which is twice as high as the yield reported before [18,36]. The ^{1}H-and ^{13}C-NMR values are given in the Experimental section. One set of pyridyl signals could be observed in the ^{1}H-NMR spectrum and two triplets for the ferrocene protons at 4.83 and 4.32 ppm. Two signals are observed in the ^{13}C-NMR spectrum for the secondary ferrocene carbons at 71.6 and 68.9 ppm, while the quaternary carbon was observed at 85.5 ppm.

3.1.2. (BPF)Pd(Me)Cl (2)

Complex 2 was prepared by reaction of (COD)PD-(Me)Cl with 1.1 equivalent of the ligand BPF in toluene (Eq. (1)).

At room temperature a red precipitate is formed in 91% yield, which is air stable in solution as well as in crystalline form. The product is soluble in most polar non-coordinating solvents. In coordinating solvents such as DMSO and acetonitrile, partial dissociation of the complex occurs, as shown by NMR. The fact that substitution of the ligand occurs with acetonitrile and DMSO is an indication that BPF is not coordinated strongly to the palladium atom.

The complex was characterized by ^{1}H-, ^{13}C-NMR, elemental analysis and a single crystal X-ray structure determination.

The ^{1}H- and ^{13}C-NMR data (see Experimental section) were measured at 223 K, since at room temperature the signals of the ferrocene protons were broad. The atomic numbering is shown in Scheme 1. The two pyridyl groups of the coordinated ligand are inequivalent, from which it may be concluded that BPF coordinates in a *cis* chelating fashion, comparable with other bidentate nitrogen ligands [10,13,14,16]. The pyridyl H5 and H15 signals at 9.16 and 9.11 ppm respectively have shifted to higher ppm values when compared with the free ligand value of 8.36 ppm. The shift of H15 to a higher ppm value is normal for a proton adjacent to a chloride, while the shift of H5 close to a methyl group is rather large [37]. The other signals of the pyridyl groups remain in the same range and, because of the inequivalency of the protons, the signals overlap. A precise assignment of these protons is not possible.

The low temperature ^{1}H-NMR spectrum shows six broad singlets for the ferrocene ring protons. Two signals at 6.46 ppm and 6.63 ppm are assigned to H7 and H20 respectively. The shift of the proton signals to lower field by 2 ppm compared with the other four

Table 6
Selected bond distances (Å) in (BPF)[$PtCl_2(CH_2=CH_2)$]$_2$ (3) (with e.s.d.s in parentheses)

Pt1–Cl1	2.282(3)	C21–C22	1.36(2)	C1–C2	1.39(1)
Pt1–Cl2	2.287(4)	C23–C24	1.39(2)	C1–C6	1.49(1)
Pt1–C21	2.17(1)	C1–N1	1.33(1)	C12–C13	1.37(2)
Pt1–C22	2.13(2)	C2–C3	1.39(2)	C13–C14	1.35(2)
Pt1–N1	2.079(8)	C3–C4	1.36(2)	C14–C15	1.35(2)
Pt2–Cl3	2.296(3)	C4–C5	1.38(2)	C15–N2	1.37(1)
Pt2–Cl4	2.292(4)	C5–N1	1.33(1)		
Pt2–C23	2.17(1)	C11–C12	1.40(1)		
Pt2–C24	2.16(1)	C11–C16	1.49(1)		
Pt2–N2	2.073(8)	C11–N2	1.33(1)		

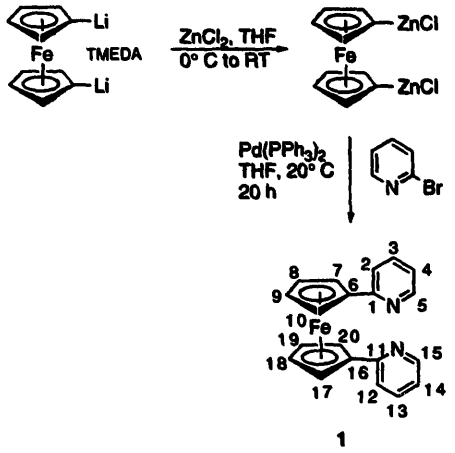

Scheme 1.

signals of the ferrocene protons may be due to the inductive effect of the metal halide [38]. The other four signals at 4.65, 4.58, 4.51 and 4.43 ppm, with the intensity of two protons which originate from the other ferrocenyl protons, could not be assigned unequivocally. The proton NMR signals of the methyl group σ-bonded to the palladium are observed at 0.91 ppm in the ^{1}H-NMR spectrum and the ^{13}C-signal of this methyl at −6.29 ppm in the ^{13}C-NMR spectrum, which is as expected [37]. In the ^{13}C-NMR spectrum ten different pyridyl and ten ferrocene signals could be observed. Most of the pyridyl and ferrocene carbon signals were shifted 1–2 ppm to higher values upon coordination.

3.1.3. $BPF[PtCl_2(CH_2=CH_2)]_2$ (3)

In an attempt to synthesize a monomeric $PtCl_2$ complex with a chelating BPF ligand in the reaction of the ligand with Zeise's salt in CH_2Cl_2 another product, **3**, was formed in 82% yield (Eq. (2)).

The red product **3** is very stable in air and soluble in various polar solvents such as dichloromethane, chloroform and methanol. In this complex two $PtCl_2(CH_2=CH_2)$ fragments are bridged by one BPF ligand. Attempts to dissociate the coordinated ethylene from the metal in hot methanol failed, while reactions with silver salts like AgOTf led to uncharacterizable products.

Complex **3** was characterized by ^{1}H-, ^{13}C-NMR, elemental analysis and a single crystal X-ray structure determination.

In the ^{1}H-NMR spectrum one signal at 4.73 ppm ($^2J_{Pt-H}$ = 62 Hz) with an intensity of eight protons was

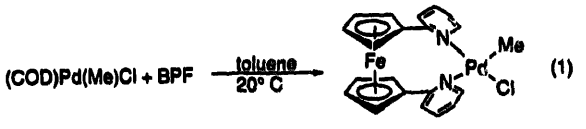

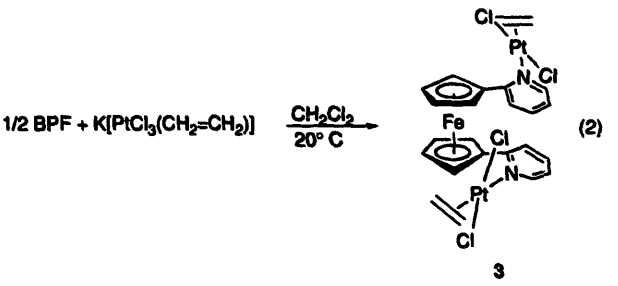

observed for ethylene, η^2-coordinated towards the metal. The olefinic protons of the complex Pt_2Cl_4(E-CH_3CH=$CHCH_3)_2$(^{i}PrN=CHCH=N^{i}Pr) [39], which has a similar structure to complex **3**, show $^2J_{Pt-H}$ = 60 Hz. This coupling constant is common for a four-coordinate planar complex [40]. Two triplets at 4.67 and 5.75 ppm originate from the ferrocene protons. The signal at 5.75 ppm shifts to a higher ppm value because of the inductive effects of the metal [38]. The equivalent H3 and H13 signals of the pyridyl rings at 7.56 ppm shift to a higher ppm value upon coordination, probably because these protons are pointing towards the chloride of the other Pt centre (see molecular structure, vide infra). The equivalent signals of H5 and H15 of the pyridyl rings shift to 8.48 ppm with $^3J_{Pt-H}$ = 30 Hz, which is characteristic of pyridyl–Pt complexes [41].

In the ^{13}C-NMR spectrum the equivalent C3 and C13 signals shift from 120 ppm in the free ligand to 129.5 ppm, while the η^2-coordinated ethylene ^{13}C-NMR signals resonate at 74.4 ppm, which is common in such complexes [42].

3.2. Molecular structure of 2

A view of the molecular structure of the complex **2** is shown in Fig. 1. Tables 3 and 4 contain the bond lengths and bond angles of the non-hydrogen atoms respectively.

This molecular structure clearly shows the bidentate coordination of the nitrogen ligand to the palladium metal with the two other ligands, methyl and chloride, completing the coordination plane. The palladium to ligand distances are as expected. The Pd–N2 distance of 2.197(3) Å is longer than Pd–N1 (2.074(4) Å) because of the higher *trans* influence of the methyl group [43]. A very interesting feature of this structure is the bite angle N1–Pd–N2 of 84.48(13)°, which is appreciably larger than in comparable complexes of this type containing α-diimine ligands [13]. The bite angle is half as large as the bite angle of this ligand in the complex $[Ag(BPF)ClO_4]_2$ [17]. In the latter complex the ligand acts nearly as a *trans*-chelating ligand (N1–Ag–N2 = 163.1(2)°) and possesses C_2 symmetry, while in complex **2** the symmetry of the ligand is C_s. The occurrence

Table 7
Selected bond angles in (BPF)[$PtCl_2(CH_2=CH_2)$]$_2$ (3) (with e.s.ds in parentheses)

Cl1–Pt–C12	176.9(1)	C14–Pt2–C23	91.10(4)	C13–C14–C15	119(1)
Cl1–Pt1–C21	90.9(4)	C14–Pt2–C24	91.8(4)	C14–C15–N2	124(1)
Cl1–Pt1–C22	89.9(6)	C14–Pt–N2	89.2(2)	Pt1–C21–C22	70(1)
Cl1–Pt1–N1	90.3(3)	C23–Pt2–C24	37.6(5)	Pt1–C22–C21	73(1)
Cl2–Pt1–C21	90.0(5)	C23–Pt2–N2	161.6(4)	Pt2–C23–C24	70.9(8)
Cl2–Pt1–C22	92.6(6)	C24–Pt2–N2	160.8(4)	Pt2–C24–C23	71.6(8)
Cl2–Pt1–N1	87.8(3)	C2–C1–N1	120.5(8)	Pt1–N1–C1	122.5(6)
C21–Pt1–C22	37.0(7)	C1–C2–C3	120(1)	Pt1–N1–C5	117.4(7)
C21–Pt1–N1	162.2(5)	C2–C3–C4	118(1)	C1–N1–C5	119.9(9)
C22–Pt1–N1	160.8(5)	C3–C4–C5	120(1)	Pt2–N2–C11	124.4(6)
C13–Pt2–C14	176.2(1)	C4–C5–N1	122(1)	Pt2–N2–C15	118.4(6)
C13–Pt2–C23	90.4(4)	C12–C11–N2	120.2(8)	C11–N2–C15	117.0(8)
C13–Pt2–C24	91.5(4)	C11–C12–C13	121(1)	C12–C13–C14	118(1)
C13–Pt–N2	88.4(2)				

of both small and large bite angles indicates that the ligand is very flexible indeed. The two symmetries, C_2 and C_s, however, might not interconvert very easily when the ligand is coordinated to a metal centre, because of a possibly high activation energy between the two states.

The least-square planes through the two pyridyl groups are perpendicular to that formed by N1–Pd–N2. The two cyclopentadienyl rings of the ferrocene backbone make a dihedral angle of 3.3(2)°, which is smaller than that in the complex $[Ag(BPF)ClO_4]_2$, for which an angle of 7.6(4)° was found.

3.3. Molecular structure of 3

A view of the molecular structure of the complex **3** is shown in Fig. 2. Tables 6 and 7 contain the bond lengths and bond angles of the non-hydrogen atoms respectively.

In this structure it can be seen that the platinum centres are in a virtually planar surrounding. The angles of Cl–Pt–N do not deviate much from 90°, while the ethylene groups are perpendicular to the coordination plane. The angles of Cl(1)–Pt(1)–Cl(2) and Cl(3)–Pt(2)–Cl(4) (176.9° and 176.2° respectively) are slightly distorted from linearity probably because of packing effects. The pyridyl(1) and pyridyl(2) planes make an angle of 100.6°(3) and 74.7°(3) with the coordination planes of Pt(1) and Pt(2) respectively. These deviations may be caused by interaction of the chloride with the ferrocenyl backbone. The two pyridyl planes are almost coplanar and make an angle of 19° with one another. The average distance between the atoms of the two rings is 3.65 Å, which indicates that the two pyridyl rings are held together by π-stacking. The Pt-N and Pt–Cl distances are in the range observed for other four-coordinated platinum complexes [39,44–47].

A dinuclear complex is formed because the strong coordination of the ethylene group results in only one coordination site. Furthermore, rotation around the ferrocenyl C_5H_4–pyridyl axes alleviates steric hindrance and the two pyridyl groups form a bridge between two platinum atoms.

3.4. Reaction of (BPF)Pd(Me)Cl with CO

A rapid and almost quantitative CO insertion into the palladium–methyl bond of complex **2** occurs to give

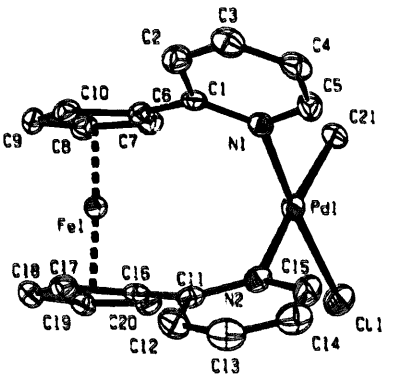

Fig. 1. An ORTEP [24] plot at 50% probability level of complex (BPF)Pd(Me)Cl (2); hydrogen atoms and CH_2Cl_2 omitted for clarity.

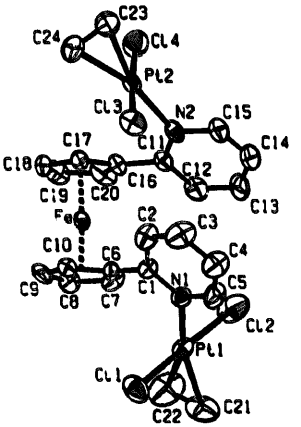

Fig. 2. An ORTEP [24] plot at 50% probability level of complex (BPF)[$PtCl_2(H_2C=CH_2)$]$_2$ (3); hydrogen atoms and CH_2Cl_2 omitted for clarity.

(BPF)Pd(C(O)Me)Cl (3) (Eq. (3)) when CO is bubbled through a solution of 2 in dichloromethane for 5 min at 294 K. This CO insertion is comparable with other complexes containing bidentate nitrogen ligands [13].

The red crystalline product which was obtained in 90% yield is air stable in solution and as a solid. The complex is soluble in polar non-coordinating solvents such as dichloromethane, while partial dissociation of the complex occurs in coordinating solvents such as acetonitrile, as has also been observed for complex 2.

The ^{1}H- and ^{13}C-NMR data were measured at 219 K because the signals are broadened at room temperature. The pattern of the ^{1}H-NMR spectrum of complex 4 is almost the same as the spectrum of 2. Upon CO insertion the methyl signal is shifted from 0.91 to 2.78 ppm [10,13], while the signals of H7 and H20 are shifted 0.15 ppm to higher values compared with the starting complex.

In the ^{13}C-NMR spectrum the ten different pyridyl and ten ferrocene signals observed did not differ much from the signals of 2. Upon CO insertion the methyl signal shifts from −6.2 to 35.7 ppm. The quaternary carbon of the CO was observed at 226.9 ppm as expected [10,13]. In the IR spectrum in KBr the CO stretching absorption could be distinguished at 1690 cm^{-1}, which is indicative of the presence of a palladium-bonded acetyl group [10,13].

Interesting behaviour was found for the complex (BPF)Pd(C(O)Me)Cl (4) under a ^{13}CO atmosphere in an NMR tube at 223 K. In the ^{1}H-NMR spectrum, besides complex 4 and free ligand, two complexes with an acetyl group, but without the ligand BPF, and one complex (BPF)Pd(C(O)Me)(CO)Cl (5) containing an acetyl and the BPF ligand coordinated as a monodentate, can be observed (see Eq. (4)). The acetyl protons at 2.80, 2.76 and 2.72 ppm are split into doublets by coupling with the ^{13}C of the inserted ^{13}CO ($^{2}J_{C-H}$ = 6 Hz).

In the ^{13}C-NMR spectrum four acetyl CO at 226.8, 218.1, 214.1, 213.9 ppm and four σ-coordinated CO signals at 184.9, 174.5, 171.7 and 171.6 ppm can be observed. The acetyl CO signal at 226.9 ppm originates from complex 4 and the signal at 184.9 ppm originates from free CO.

Complex 5, in which the ligand is coordinated as a monodentate, shows a typical σ-coordinated carbonyl at 174.5 ppm [8,48,49] and an acetyl signal at 218.11 ppm. The two complexes without BPF, but both containing a Pd–CO and an acetyl at 171.9, 171.6 and 214.1, 213.9

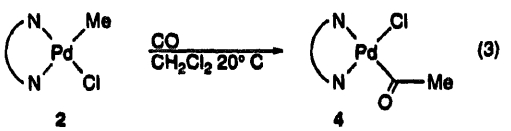

2 4 (3)

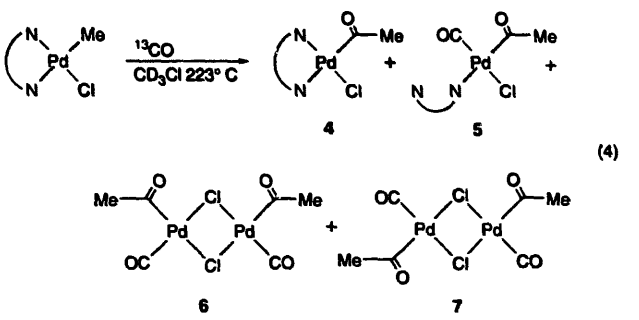

4 5 (4)

6 7

ppm respectively, are possibly two isomers of the chloride bridged dimers *cis*- and *trans*-$Pd_2(CO)_2(C(O)Me)_2Cl_2$, complexes 6 and 7.

The IR spectrum at 223 K under ^{12}CO atmosphere shows three acetyl absorptions at 1736, 1669 and 1693 cm^{-1}, of which the last absorption is due to complex 4 as has been mentioned before. In the σ-carbonyl region only one absorption can be observed at 2105 cm^{-1}, while three signals would be expected. The three σ-carbonyl absorptions overlap around 2105 cm^{-1} in the IR spectrum.

It is difficult to compare the IR values with other complexes known in the literature. The value of 2105 cm^{-1} is lower than that for the cationic complex $[Pd(C_6F_5)(CO)L_2]^+$ (2132–2163 cm^{-1}) [50] or for the neutral complex $[Pd(C_6F_5)_2(CO)_2]$ (2152–2186 cm^{-1}) [51]. It is also lower than that for the chloride bridged complex $Pd_2Cl_4(CO)_2$ (2163 cm^{-1}) [48] and that for the anionic complex $[PdCl_3(CO)]^-$ (2146 cm^{-1}). The value of 2105 cm^{-1} is analogous to values found for the anionic complexes $[PPh_3(CH_2Ph)][Pd(R)Cl_2(CO)]$ (2100, 2115 cm^{-1}), which may be explained by a relatively high π-back donation from the metal to the CO [52].

The easy dissociation of the BPF ligand of complex 4 in coordinating solvents and in the presence of CO indicates again that the ligand is not coordinating very strongly to the metal centre.

3.5. Fluxionality of complexes 2 and 4

The fluxionality of the complexes 2 and 4 was investigated with variable temperature ^{1}H-NMR spectroscopy. The variable temperature ^{1}H-NMR spectra of 2 show that the temperature only influences the ferrocenyl signals and not the signals of the pyridyl group (see Fig. 3), which remain non-equivalent also at higher temperatures. At elevated temperatures some decomposition of the complex occurs, which explains the appearance of some free ligand at 340 K.

The coalescence of the signals of the ferrocenyl protons H7 with H10, H17 with H20, H8 with H9 and H18 with H19 can only be explained by the fluxional

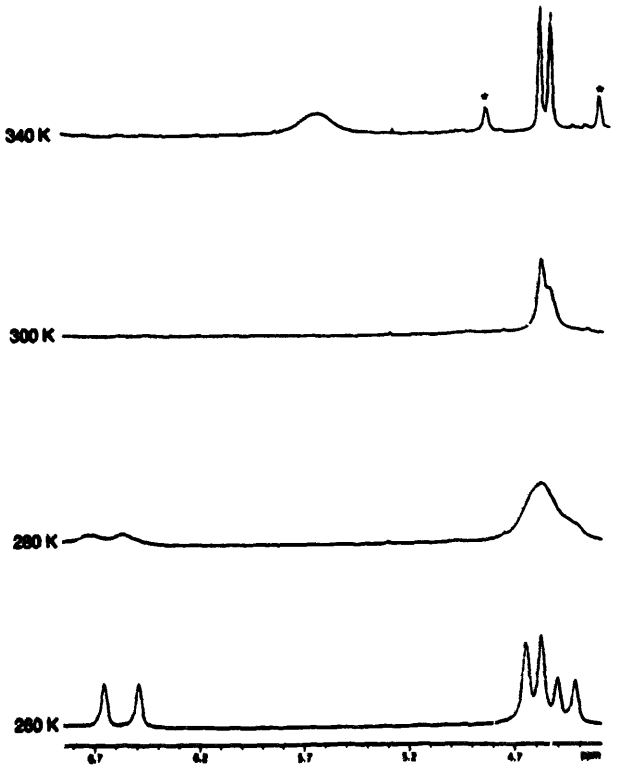

Fig. 3. Variable temperature ^{1}H-NMR spectra of (BPF)Pd(Me)Cl (2) in $CDCl_3$ (* denotes free BPF signal).

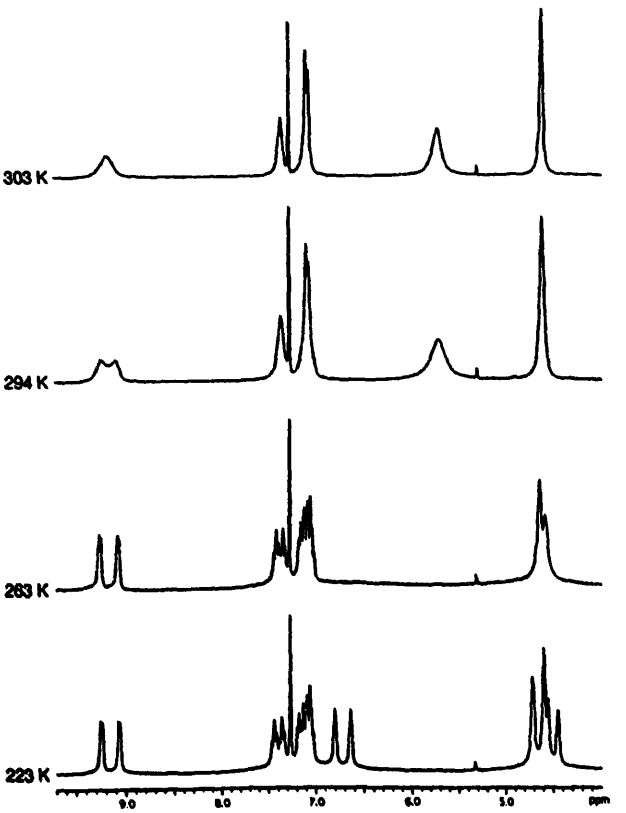

Fig. 5. Variable temperature ^{1}H-NMR spectra of (BPF)Pd(C(O)Me)Cl (4) in $CDCl_3$.

process shown in Fig. 4. The two enantiomers interchange by a rotation around both C_5H_4–pyridyl axes, while both nitrogens remain coordinated to the metal atom. Such a fluxional process has been observed earlier for [Rh(COD)(BPF)]ClO_4 and for [Fe(η^5-C_5H_4(2-C_5H_4N)(η^5-$C_5H_4PPh_2$)]Rh(COD) [17,53].

The variable temperature ^{1}H-NMR spectra of complex 4, however, show that both the ferrocenyl and pyridyl signals are involved (see Fig. 5). At low temperature two different pyridyl and two different cyclopentadienyl groups can be observed, while at high temperature the two pyridyl and two cyclopentadienyl groups are equivalent. In this exchange N_1 moves from *trans* to *cis* with regard to the chloride (see Fig. 6). This exchange may be explained either by a dissociation of one of the pyridyl groups or by a dissociation of the chloride and subsequent isomerization. In view of the weak bonding of the ligand to the metal atom in according solvents, the former possibility appears more likely.

The ^{1}H-NMR spectrum at 303 K in Fig. 5 shows two signals for the ferrocene protons, while four signals would be expected with only the fluxional behaviour of Fig. 6 taken into account. The appearance of the two signals can be explained again by a coalescence of the ferrocenyl protons H7 with H10, H17 with H20, H8 with H9 and H18 with H19, as shown in Fig. 4, identical to complex 2.

The fact that the fluxional process shown in Fig. 6 takes place in complex 4 and does not take place in complex 2 may be rationalized by the higher *trans* influence of the C(O)Me group with regard to the CH_3 group [54]. This higher *trans* influence leads to preferential weakening of the Pd–pyridyl bond *trans* to the C(O)Me group and to dissociation of the pyridyl group, whereby the rearrangement as shown in Fig. 6 becomes feasible.

The facile rearrangements occurring for the complexes 2 and 4 are further proof of the flexibility of BPF.

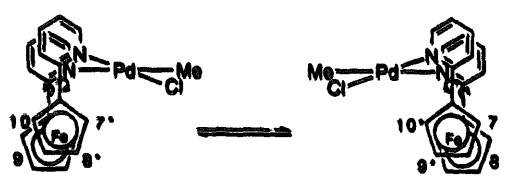

Fig. 4.

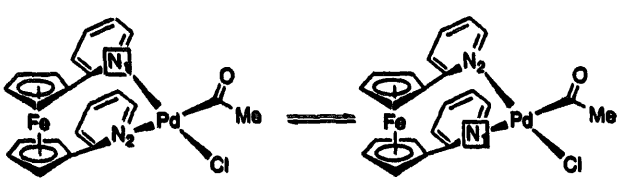

Fig. 6.

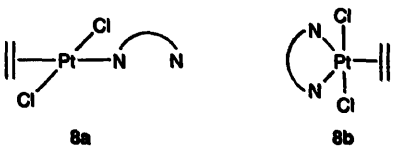

8a 8b

Fig. 7.

3.6. $BPF[PtCl_2(CH_2=CH_2)]_2$ (3) with extra ligand BPF

Upon addition of one equivalent of BPF to a solution of complex **3** in $CDCl_3$ three species can be observed in the ^{1}H-NMR spectrum, which are complex **3**, free ligand, and a new complex. Precipitation by Et_2O yielded the complex $BPF[PtCl_2(CH_2=CH_2)]_2$ (**3**) in crystalline form and free ligand in solution, while the new complex could not be isolated. The ratio of the three species in $CDCl_3$ does not very much depend on the temperature, solvent or amount of free ligand. From the ^{1}H-NMR signals, which show overlap especially in the pyridyl region, it can be deduced that in the case of the new compound only one BPF ligand is coordinated to the metal. One ethylene signal with an intensity of four protons occurs at 4.67 ppm. On the basis of these observations two structures (see Fig. 7) can be proposed, of which structure **8a** is four-coordinated with a monodentate ligand and structure **8b** is five-coordinated with a trigonal–bipyramidal configuration.

The formation of four- and five-coordinated Pt–alkene complexes has been extensively studied [39,42,44–46,55,56]. It has been reported that bidentate nitrogen ligands with a small ring size and bite angle, such as $R_2N(CH_2)_2NR_2$, stabilize five-coordinated complexes and that four-coordinated complexes will be formed with flexible ligands and a large ring size such as $R_2N(CH_2)_3NR_2$ [39]. Since BPF is a very flexible ligand and forms a large ring size it may be expected that a four-coordinated complex **8a** is the more likely proposition. Also, the ethylene signal of five-coordinated complexes is commonly observed between 3.4 and 3.6 ppm [39], while for four-coordinated complexes this value is observed at least around 4.5 ppm. Since the ethylene signal of the new complex occurs at 4.67 ppm we conclude that structure **8a** is the most likely one.

4. Conclusions

In conclusion, BPF is indeed a highly flexible ligand that can accommodate a variety of bite angles in its complexes. The insertion of carbon monoxide into the palladium–methyl bond is fast. Unfortunately, BPF binds only weakly to palladium, thus prohibiting a detailed study of the kinetics of the insertion reaction.

5. Supplementary material available

Further details of the structure determinations, including atomic coordinates, bond lengths and angles and thermal parameters for **2** and **3** (22 pages). Ordering information is given on any current masthead page.

Acknowledgements

Professor Dr. E. Drent (Koninklijke Shell-Laboratorium, Amsterdam) and Professor Dr. C.J. Elsevier are acknowledged for their helpful discussions and Shell Research BV for financial support. This work was supported in part (A.L.S. and N.V.) by the Netherlands Foundation of Chemical Research (SON) with financial aid from the Netherlands Organization for Scientific Research (NWO).

References

[1] E. Drent, *European Patent Application*, 121965, 1984.
[2] A. Sen and Z. Jiang, *Macromolecules*, *26* (1993) 911–915.
[3] A. Sen and T.-W. Lai, *J. Am. Chem. Soc.*, *104* (1982) 3520–3522.
[4] D. Roberto, M. Catellani and G.P. Chiusoli, *Tetrahedron Lett.*, *29* (1988) 2115–2118.
[5] M. Brookhart and M.I. Wagner, *J. Am. Chem. Soc.*, *116* (1994) 3641–3642.
[6] M. Barsacchi, G. Consiglio, L. Medici, G. Petrucci and U.W. Suter, *Angew. Chem., Int. Ed. Engl.*, *30* (1991) 989–991.
[7] G.P.C.M. Dekker, C.J. Elsevier, K. Vrieze and P.W.N.M. van Leeuwen, *Organometallics*, *11* (1992) 1598.
[8] I. Tóth and C.J. Elsevier, *J. Am. Chem. Soc.*, *115* (1993) 10388–10389.
[9] P.W.N.M. van Leeuwen, C.F. Roobeek and H. van der Heijden, *J. Am. Chem. Soc.*, *116* (1994) 12117–12118.
[10] R. van Asselt, E.E.C.G. Gielens, R.E. Rülke, K. Vrieze and C.J. Elsevier, *J. Am. Chem. Soc.*, *116* (1994) 977–985.
[11] G.P.C.M. Dekker, A. Buijs, C.J. Elsevier, K. Vrieze, P.W.N.M. van Leeuwen, W.J.J. Smeets, A.L. Spek, Y.F. Wang and C.H. Stam, *Organometallics*, *11* (1992) 1937–1948.
[12] R.E. Rülke, I.M. Han, C.J. Elsevier, K. Vrieze, P.W.N.M. van Leeuwen, C.F. Roobeek, M.C. Zoutberg, Y.F. Wang and C.H. Stam, *Inorg. Chim. Acta*, *169* (1990) 5–8.
[13] R.E. Rülke, J.G.P. Delis, A.M. Groot, C.J. Elsevier, P.W.N.M. van Leeuwen, K. Vrieze, K. Goubitz, H. Schenk, *J. Organomet. Chem.*, in press.
[14] W. de Graaf, J. Boersma and G. van Koten, *Organometallics*, *9* (1990) 1479.
[15] B.A. Markies, D. Kruis, M.H.P. Rietveld, K.A.N. Verkerk, J. Boersma, H. Kooijman, M.T. Lakin, A.L. Spek and G. van Koten, *J. Am. Chem. Soc.*, *117* (1995) 5263–5274.
[16] B.A. Markies, K.A.N. Verkerk, M.H.P. Rietveld, J. Boersma, H. Kooijman, A.L. Spek and G. Koten, *J. Chem. Soc., Chem. Commun.*, (1993) 1317–1319.
[17] K. Tani, T. Mihana, T. Yamagata and T. Saito, *Chem. Lett.*, (1991) 2047–2050.

[18] M.D. Rausch and D.J. Ciappenelli, *J. Organomet. Chem.*, *10* (1967) 127–136.
[19] R.E. Rülke, J.M. Ernsting, A.L. Spek, C.J. Elsevier, P.W.N.M. van Leeuwen and K. Vrieze, *Inorg. Chem.*, *32* (1993) 5769–5778.
[20] F.R. Hartley, *Organomet. Chem. Rev. A*, *6* (1970) 119–137.
[21] J.L. de Boer and A.J.M. Duisenberg, *Acta Crystallogr.*, *A40* (1984) C410.
[22] A.L. Spek, *J. Appl. Crystallogr.*, *21* (1988) 578.
[23] N. Walker and D. Stuart, *Acta Crystallogr.*, *A39* (1983) 158.
[24] A.L. Spek, *Acta Crystallogr.*, *A46* (1990) C34.
[25] P.T. Beurskens, G. Admiraal, G. Beurskens, W.P. Bosman, S. García-Granda, R.O. Gould, J.M.M. Smits and C. Smykalla, *The DIRDIFF program system*, Tech. Rep. Crystallography Laboratory, University of Nijmegen, Netherlands, 1992.
[26] G.M. Sheldrick, *SHELXL-93 Program for crystal structure refinement*, University of Göttingen, Germany, 1993.
[27] A.L. Spek, *A.C.A. Abstr.*, *22* (1994) 66.
[28] A.J.C. Wilson, *International Tables for Crystallography*, Vol. C, Kluwer Academic, Dordrecht, 1992.
[29] J.M.M. Smits, H. Behm, W.P. Bosman and P.T. Beurskens, *J. Crystallogr. Spectrosc. Res.*, *18* (1991) 447.
[30] W.H. Zachariasen, *Acta Crystallogr.*, *A23* (1967) 558.
[31] A.C. Larson, F.R. Ahmad, S.R. Hall and C.P. Huber (eds.) *Crystallographic Computing*, Munksgaard, Copenhagen, 1969, pp. 291–294.
[32] *International Tables for X-ray Crystallography*, Vol. IV, Kynoch Press, Birmingham, 1974, p. 5.
[33] D.T. Cromer and J.B. Mann, *Acta Crystallogr.*, *A24* (1968) 321–324.
[34] S.R. Hall, H.D. Flack and J.M. Stewart, *XTAL3.2 Reference Manual*, Universities of Western Australia, Geneva and Maryland, 1992.
[35] M.E. Huttenloch, J. Diebold and H.H. Brintzinger, *Organometallics*, *11* (1992) 3600–3607.
[36] K. Schlögl and M. Fried, *Monatsh. Chem.*, *94* (1963) 537–543.
[37] P.K. Byers and A. Canty, *Organometallics*, *9* (1990) 210–220.
[38] B. McCulloch, D.L. Ward, J.D. Woollins and C.H.J. Brubaker, Jr., *Organometallics*, *4* (1985) 1425–1432.
[39] V.G. Albano, F. Demartin, A. De Renzi, G. Morelli and A. Saporito, *Inorg. Chem.*, *24* (1985) 2032–2039.
[40] M.E. Cucciolito, V. De Felice, A. Panunzi and A. Vitagliano, *Organometallics*, *8* (1989) 1180–1187.
[41] E. Bielli, P.M. Gillard and B.T. Heaton, *J. Chem. Soc., Chem. Commun.*, (1974) 2133–2139.
[42] V.G. Albano, G. Natile and A. Panunzi, *Coord. Chem. Rev.*, *133* (1994) 67–114.
[43] T.G. Appleton, H.C. Clark and L.E. Manzer, *Coord. Chem. Rev.*, *10* (1973) 335.
[44] F.P. Fanizzi, F.P. Intini, L. Maresca, G. Natile, M. Lanfranchi and A. Tiripicchio, *J. Chem. Soc., Dalton Trans.*, (1991) 1007–1015.
[45] F.P. Fanizzi, L. Maresca, G. Natile, M. Lanfranchi, A. Tiripicchio and G. Pacchioni, *J. Chem. Soc., Chem. Commun.*, (1992) 333–335.
[46] G. Gervasio, S.A. Mason, L. Maresca and G. Natile, *Inorg. Chem.*, *25* (1986) 2207–2211.
[47] R.S. Osborn and D. Rogers, *J. Chem. Soc., Chem. Commun.*, (1974) 1002–1004.
[48] F. Calderazzo and D. Belli Dell'Amico, *Inorg. Chem.*, *20* (1981) 1310.
[49] J. Browning, P.L. Goggin, R.J. Goodfellow, M.G. Norton, A.J.M. Rattray, B.F. Taylor and J. Mink, *J. Chem. Soc., Dalton Trans.*, (1977) 2061–2067.
[50] R. Uson, J. Fornies and F. Martinez, *J. Organomet. Chem.*, *112* (1976) 105–110.
[51] R. Uson, J. Fornies, M. Tomas and B. Menjon, *Organometallics*, *4* (1985) 1912–1914.
[52] J. Vicente, A. Arcas, M.V. Borrachero, A. Tiripicchio and M. Tiripicchio Camellini, *Organometallics*, *10* (1991) 3873–3876.
[53] T. Yoshida, K. Tani, T. Yamagata, Y. Tatsuno and T. Saito, *J. Chem. Soc., Chem. Commun.*, (1990) 292–294.
[54] J.T. Chen, Y.S. Yeh, C.S. Yang, F.Y. Tsai, G.L. Huang, B.C. Shu, T.M. Huang, Y.S. Chen, G.H. Lee, M.C. Cheng, C.C. Wang and Y. Wang, *Organometallics*, *13* (1994) 4804–4824.
[55] H. van der Poel, G. van Koten, K. Vrieze, M. Kokkes and C.H. Stam, *J. Organomet. Chem.*, *175* (1979) C21–C24.
[56] H. van der Poel, G. van Koten and K. Vrieze, *Inorg. Chem.*, *19* (1980) 1145–1151.